

## **Supplementary Materials**

**Whole-Exome and RNA-Sequencing Analyses of Acinic Cell Carcinomas of the Breast**

**Beca et al.**

**Supplementary Methods**

**Supplementary Figure 1**

**Supplementary Tables 1-5**

## **SUPPLEMENTARY METHODS**

### **Subjects and samples**

Following Institutional Review Boards approval formalin-fixed paraffin embedded tissue blocks of acinic cell carcinomas (ACCs) of the breast were retrieved from the archives of the Department of Pathology of the Nottingham City Hospital/Nottingham University Hospitals NHS Trust. Estrogen receptor (ER) and HER2 status was evaluated following the ASCO/CAP guidelines<sup>1,2</sup>. Informed consent was obtained according to the the protocol approved by the local Institutional Review Board (IRB). Cases were reviewed by three pathologists (E.P., E.G-R. and J.S.R.F.), classified as breast ACCs following the criteria put forward by the World Health Organization<sup>3</sup>, and graded according to the Nottingham grading system<sup>4</sup>. Immunohistochemical assessment of MLH1 expression was performed on a Leica Bond III automated stainer platform (Leica, Buffalo Grove, IL) using the anti-MLH1 monoclonal antibody (clone ES05; catalogue #: 26408; Leica Biosystems, Newcastle, UK) at a 1:500 dilution for 30 minutes following EDTA-based high pH epitope retrieval. The standard platform-associated polymeric detection kit (Refine, Leica) was used as secondary reagent. Positive and negative controls were included in each slide run. For MLH1 immunohistochemical analysis, a case was considered interpretable if MLH1 expression could be detected in stromal and/or inflammatory cells (i.e. internal positive control).

### **Whole-exome sequencing analysis**

DNA samples derived from microdissected tumor and normal tissue from ACCs were subjected to whole-exome sequencing (WES) at the Integrated Genomics Operations (IGO) of Memorial Sloan Kettering Cancer Center (MSKCC) using validated protocols, as previously described.<sup>5,6</sup> Reads were aligned to the reference human genome GRCh37 using the Burrows-Wheeler Aligner (BWA, v.0.7.10)<sup>7</sup>. Local realignment, duplicate removal, and base quality recalibration were performed using the Genome Analysis Toolkit (GATK, v3.1.1).<sup>8</sup> Sequencing

data were analyzed as previously described.<sup>5, 6</sup> In brief, somatic single nucleotide variants (SNVs) were detected by MuTect (v1.0.0)<sup>9</sup>, small insertion and deletion (indels) by Strelka (v.2.0.15),<sup>10</sup> VarScan2 (v.2.3.7),<sup>11</sup> Lancet (v1.0.0)<sup>12</sup> and Scalpel (v0.5.53)<sup>13</sup>. SNVs and indels with a >1% global minor allele frequency in ExAC<sup>14</sup> were excluded. We additionally filtered for the FFPE pooled normal passenger mutations by 1) removing mutations with > 1% global minor allele frequency in gnomAD<sup>15</sup>, 2) removing the mutations with a normal locus depth of less than 10 and 3) include only mutation in both gnomAD and ExAC. ABSOLUTE (v1.0.6)<sup>16</sup> was employed to determine the cancer cell fraction (CCF) of each mutation. FACETS<sup>17</sup> was used to determine copy number alterations and whether genes harboring a somatic mutation were targeted by loss of heterozygosity as previously described<sup>5, 6</sup>. Large-scale state transitions (LST) score<sup>18</sup>, NtAI score<sup>19</sup> and Myriad score<sup>20</sup> were calculated as genomic features of homologous recombination DNA repair deficiency as previously described<sup>21</sup>. Mutations affecting hotspot codons were annotated according to Chang et al.<sup>22</sup> Mutational signatures were defined using Sigma Multivariate Analysis (SigMA)<sup>23</sup> using all synonymous and non-synonymous mutations. Microsatellite instability was quantified using MSIsensor<sup>24</sup>, as previously described<sup>25</sup>.

### **RNA-sequencing and fusion gene identification**

RNA extracted from all three ACCs included in this study was subjected to RNA-sequencing at MSK's IGO using validated protocols<sup>26, 27</sup>. In brief, paired-end RNA-sequencing was performed with 2x100 bp cycles on an Illumina HiSeq2000. We identified read pairs supporting fusion transcripts using INTEGRATE<sup>28</sup>, deFuse<sup>29</sup> and FusionCatcher<sup>30</sup>. Fusion genes and read-through candidates that were detected in a set of 297 normal samples from The Cancer Genome Atlas (TCGA)<sup>31</sup> were excluded to account for alignment artifacts and normal transcriptional variants. Remaining candidate fusions were annotated using OncoFuse<sup>32</sup> to define their oncogenic potential. Additionally, the presence of candidate fusion

genes was inferred on the tumor fusion gene data portal<sup>33</sup>, which comprises a list of 20,731 fusion genes across 33 cancer types (n=9,950).

## SUPPLEMENTARY REFERENCES

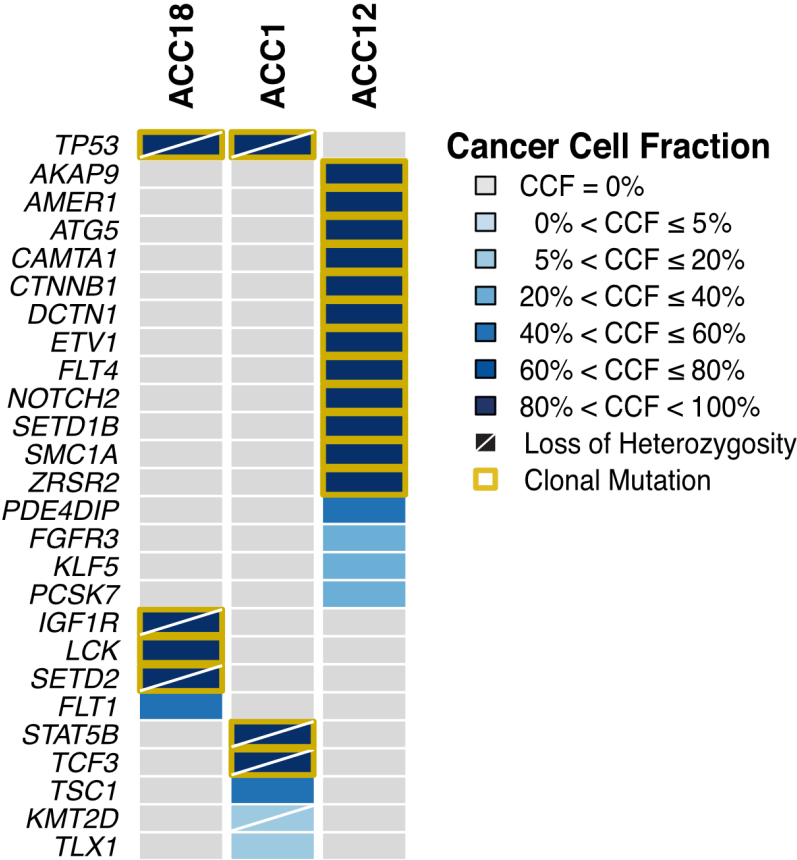
1. Wolff AC, Hammond MEH, Allison KH *et al.* Human epidermal growth factor receptor 2 testing in breast cancer: American society of clinical oncology/college of american pathologists clinical practice guideline focused update. *Arch Pathol Lab Med* 2018;**142**;1364-1382.
2. Hammond ME, Hayes DF, Dowsett M *et al.* American society of clinical oncology/college of american pathologists guideline recommendations for immunohistochemical testing of estrogen and progesterone receptors in breast cancer. *J Clin Oncol* 2010;**28**;2784-2795.
3. Lakhani SR, Ellis IO, Schnitt SJ, Tan PH, van de Vijver MJ. *Who classification of breast tumors*. IARC: Lyon, 2012.
4. Elston CW, Ellis IO. Pathological prognostic factors in breast cancer. I. The value of histological grade in breast cancer: Experience from a large study with long-term follow-up. *Histopathology* 1991;**19**;403-410.
5. Pareja F, Brandes AH, Basili T *et al.* Loss-of-function mutations in atp6ap1 and atp6ap2 in granular cell tumors. *Nat Commun* 2018;**9**;3533.
6. Geyer FC, Li A, Papanastasiou AD *et al.* Recurrent hotspot mutations in hras q61 and pi3k-akt pathway genes as drivers of breast adenomyoepitheliomas. *Nat Commun* 2018;**9**;1816.
7. Li H, Durbin R. Fast and accurate long-read alignment with burrows-wheeler transform. *Bioinformatics* 2010;**26**;589-595.
8. McKenna A, Hanna M, Banks E *et al.* The genome analysis toolkit: A mapreduce framework for analyzing next-generation DNA sequencing data. *Genome Res* 2010;**20**;1297-1303.
9. Cibulskis K, Lawrence MS, Carter SL *et al.* Sensitive detection of somatic point mutations in impure and heterogeneous cancer samples. *Nat Biotechnol* 2013;**31**;213-219.

10. Saunders CT, Wong WS, Swamy S, Becq J, Murray LJ, Cheetham RK. Strelka: Accurate somatic small-variant calling from sequenced tumor-normal sample pairs. *Bioinformatics* 2012;**28**;1811-1817.
11. Koboldt DC, Zhang Q, Larson DE *et al.* VarScan 2: Somatic mutation and copy number alteration discovery in cancer by exome sequencing. *Genome Res* 2012;**22**;568-576.
12. Narzisi G, Corvelo A, Arora K *et al.* Genome-wide somatic variant calling using localized colored de bruijn graphs. *Commun Biol* 2018;**1**;20.
13. Narzisi G, O'Rawe JA, Iossifov I *et al.* Accurate de novo and transmitted indel detection in exome-capture data using microassembly. *Nat Methods* 2014;**11**;1033-1036.
14. Lek M, Karczewski KJ, Minikel EV *et al.* Analysis of protein-coding genetic variation in 60,706 humans. *Nature* 2016;**536**;285-291.
15. Karczewski KJ, Francioli LC, Tiao G *et al.* Variation across 141,456 human exomes and genomes reveals the spectrum of loss-of-function intolerance across human protein-coding genes. *bioRxiv* 2019.
16. Carter SL, Cibulskis K, Helman E *et al.* Absolute quantification of somatic DNA alterations in human cancer. *Nat Biotechnol* 2012;**30**;413-421.
17. Shen R, Seshan VE. Facets: Allele-specific copy number and clonal heterogeneity analysis tool for high-throughput DNA sequencing. *Nucleic Acids Res* 2016;**44**;e131.
18. Popova T, Manie E, Rieunier G *et al.* Ploidy and large-scale genomic instability consistently identify basal-like breast carcinomas with brca1/2 inactivation. *Cancer Res* 2012;**72**;5454-5462.
19. Birkbak NJ, Wang ZC, Kim JY *et al.* Telomeric allelic imbalance indicates defective DNA repair and sensitivity to DNA-damaging agents. *Cancer Discov* 2012;**2**;366-375.
20. Telli ML, Timms KM, Reid J *et al.* Homologous recombination deficiency (hrd) score predicts response to platinum-containing neoadjuvant chemotherapy in patients with triple-negative breast cancer. *Clin Cancer Res* 2016;**22**;3764-3773.

21. Mutter RW, Riaz N, Ng CK *et al.* Bi-allelic alterations in DNA repair genes underpin homologous recombination DNA repair defects in breast cancer. *J Pathol* 2017;**242**;165-177.
22. Chang MT, Bhattarai TS, Schram AM *et al.* Accelerating discovery of functional mutant alleles in cancer. *Cancer Discov* 2018;**8**;174-183.
23. Gulhan DC, Lee JJ, Melloni GEM, Cortes-Ciriano I, Park PJ. Detecting the mutational signature of homologous recombination deficiency in clinical samples. *Nat Genet* 2019;**51**;912-919.
24. Niu B, Ye K, Zhang Q *et al.* Msisensor: Microsatellite instability detection using paired tumor-normal sequence data. *Bioinformatics* 2014;**30**;1015-1016.
25. Ashley CW, Da Cruz Paula A, Kumar R *et al.* Analysis of mutational signatures in primary and metastatic endometrial cancer reveals distinct patterns of DNA repair defects and shifts during tumor progression. *Gynecol Oncol* 2019;**152**;11-19.
26. Pareja F, Lee JY, Brown DN *et al.* The genomic landscape of mucinous breast cancer. *J Natl Cancer Inst* 2019.
27. Geyer FC, Burke KA, Piscuoglio S *et al.* Genetic analysis of uterine adenosarcomas and phyllodes tumors of the breast. *Mol Oncol* 2017;**11**;913-926.
28. Zhang J, White NM, Schmidt HK *et al.* Integrate: Gene fusion discovery using whole genome and transcriptome data. *Genome Res* 2016;**26**;108-118.
29. McPherson A, Hormozdiari F, Zayed A *et al.* Defuse: An algorithm for gene fusion discovery in tumor rna-seq data. *PLoS Comput Biol* 2011;**7**;e1001138.
30. Edgren H, Murumagi A, Kangaspeska S *et al.* Identification of fusion genes in breast cancer by paired-end rna-sequencing. *Genome Biol* 2011;**12**;R6.
31. Cancer Genome Atlas N. Comprehensive molecular portraits of human breast tumours. *Nature* 2012;**490**;61-70.

32. Shugay M, Ortiz de Mendibil I, Vizmanos JL, Novo FJ. Oncofuse: A computational framework for the prediction of the oncogenic potential of gene fusions. *Bioinformatics* 2013;**29**;2539-2546.
33. Hu X, Wang Q, Tang M *et al.* Tumorfusions: An integrative resource for cancer-associated transcript fusions. *Nucleic Acids Res* 2018;**46**;D1144-D1149.

Supplementary Figure 1



**Supplementary Figure 1. Cancer cell fractions of non-synonymous somatic mutations affecting cancer-related genes identified in the Acinic Cell Carcinomas (ACCs) of the breast by whole-exome sequencing.** Cancer cell fractions (CCFs) and clonality of non-synonymous somatic mutations affecting cancer related genes identified in ACCs (n=3) using whole-exome sequencing. Clonal mutations are depicted by a yellow box.



**Supplementary Table 1. Clinicopathologic characteristics of the Acinic Cell Carcinomas of the breast included in this study**

Case ID	Age at diagnosis (years)	Growth pattern	Tubule formation	Nuclear pleomorphism	Mitotic count	Histologic grade*	ER status	HER2 status (IHC/FISH)
ACC1	49	Microglandular	1	3	1	1	Negative	Negative
ACC12	42	Microglandular	2	2	1	1	Negative	Negative
ACC18	N/A	Microglandular and hypernephroid	1	1	1	1	Negative	Negative

\*Nottingham grading system. ER, estrogen receptor; FISH, fluorescence *in situ* hybridization; IHC, immunohistochemistry; N/A, not available.

**Supplementary Table 2: Fusion genes identified by RNA-sequencing analysis of Acinic Cell Carcinomas of the breast**

Case ID	Fusion Caller	5' Gene	3' Gene	5' Mapping	3' Mapping	Fusion Type	Crossing Reads	Encompassing Reads	In Frame	Driver Probability (Oncofuse)	TCGA fusion data portal
ACC1T	STAR-Integrate	<i>PIK3AP1</i>	<i>CRTAC1</i>	chr10: 98376396-	chr10: 99771094-	Intra-Chromosomal	4	11	No	0.03893	Absent
ACC1T	STAR-Integrate, Defuse	<i>SLC12A2</i>	<i>PRRC1</i>	chr5: 127450371+	chr5: 126859150+	Intra-Chromosomal	1	7	No	0.28698	Absent
ACC1T	STAR-Integrate	<i>ZNF432</i>	<i>ZNF841</i>	chr19: 52543737-	chr19: 52570859-	Intra-Chromosomal	1	7	No	0.83258	Absent
ACC1T	STAR-Integrate	<i>PTGES3L-AARSD1</i>	<i>BRCA1</i>	chr17: 41116123-	chr17: 41258550-	Intra-Chromosomal	1	4	No	0.52748	Absent
ACC1T	STAR-Integrate	<i>PRRC2C</i>	<i>GORAB</i>	chr1: 171454873+	chr1: 170508350+	Intra-Chromosomal	1	2	No	0.02169	Absent
ACC1T	STAR-Integrate	<i>TC2N</i>	<i>FBLN5</i>	chr14: 92302712-	chr14: 92403542-	Intra-Chromosomal	1	2	No	0.19163	Present (Breast cancer, 2/1119)
ACC1T	Defuse	<i>JMJD1C</i>	<i>REEP3</i>	chr10: 65140239-	chr10: 65281495-	Intra-Chromosomal	7	13	No	0.07933	Absent
ACC1T	Defuse	<i>URI1</i>	<i>LTBP4</i>	chr19: 30453087+	chr19: 41111646-	Intra-Chromosomal	7	9	No	0.0232	Absent

**Supplementary Table 3: Whole-exome sequencing statistics.**

<b>Case ID</b>	<b>Tissue type (Sample ID)</b>	<b>Total reads</b>	<b>Mean target coverage (X)</b>	<b>Target bases 2X</b>	<b>Target bases 50X</b>	<b>Target bases 100X</b>
ACC1	Tumor (ACC1-T)	316,773,539	276.31	99.84	97.27	88.57
	Normal (ACC1-N)	108,277,019	22.01	99.53	02.40	00.01
ACC12	Tumor (ACC12-T)	267,776,663	107.52	99.73	87.51	54.14
	Normal (ACC12-N)	181,406,979	90.96	99.80	74.66	39.57
ACC18	Tumor (ACC18-T)	268,448,663	226.98	99.82	97.26	87.97
	Normal (ACC18-N)	158,170,351	115.07	99.79	74.66	39.57

Supplementary Table 4: Non-synonymous somatic mutations identified in the Acinic Cell Carcinomas of the breast by whole-exome sequencing.

Sample ID	Oncogene	Amplification	Chromosomes	Genomic position	Reference allele	Alternate allele	Type of mutation	Depth of mutation (%)	Mutational fraction	HOTSPOT	Cancer Cell Fraction (CCF)	Probability of false discovery rate	Upper bound of 95% confidence interval for CCF	Lower bound of 95% confidence interval for CCF	Clonal status	Mutation status	CHAM (Breast)	PROVAX	FATHMM	Loss of heterozygosity (LOH)	Pathogenicity	Cancer Gene Census	Kaoudi et al	Cancer908 genes (Lawrence et al)
ACC12T	LRIG4	p.R537G	1	1097704	G	C	Missense	104	23.1%		0.71227	0.71227	0.71227	Clonal	D						Passenger	No	No	No
ACC12T	CAMTA1	p.T363M	1	772735	C	T	Missense	104	23.1%		0.71227	0.71227	0.71227	Clonal	D						Passenger	No	No	No
ACC12T	ERE	p.R404G	1	842805	T	C	Missense	65	24.8%		0.78155	0.78155	0.78155	Clonal	D						Passenger	No	No	No
ACC12T	MEB	p.M69I	1	1017669	A	G	Missense	71	17.3%		0.88133	0.88133	0.88133	Clonal	D						Passenger	No	No	No
ACC12T	MFN2	p.F537V	1	1205881	A	T	Missense	76	19.0%		0.85617	0.85617	0.85617	Clonal	D						Passenger	No	No	No
ACC12T	C11orf134	p.G18E	1	185988	C	T	Missense	45	11.1%		0.12729	0.12729	0.12729	Subclonal	N						Passenger	No	No	No
ACC12T	CROCC	p.R603S	1	1096708	C	T	Missense	51	12.2%		0.17209	0.17209	0.17209	Subclonal	D						Passenger	No	No	No
ACC12T	GRH3	p.R408I	1	2467408	C	A	Missense	47	11.1%		0.14827	0.14827	0.14827	Clonal	N						Passenger	No	No	No
ACC12T	CTZ	p.L276I	1	1058230	C	T	Missense	47	11.1%		0.14827	0.14827	0.14827	Clonal	N						Passenger	No	No	No
ACC12T	CCDC17	p.E10G	1	4409563	C	G	Missense	69	16.0%		0.02667	0.02667	0.02667	Clonal	N						Passenger	No	No	No
ACC12T	BRIN5	p.R198H	1	4622474	C	G	Missense	97	18.8%		0.42736	0.42736	0.42736	Subclonal	D						Passenger	No	No	No
ACC12T	CCZ1B5	p.H96Y	1	1589160	C	T	Missense	39	47.2%		0.94923	0.94923	0.94923	Clonal	D						Passenger	No	No	No
ACC12T	TRCC2	p.L440V	1	8524427	G	A	Missense	59	28.0%		0.48613	0.48613	0.48613	Clonal	D						Passenger	No	No	No
ACC12T	PKM1	p.K246E	1	11089912	G	A	Missense	59	28.0%		0.48613	0.48613	0.48613	Clonal	D						Passenger	No	No	No
ACC12T	NOTCH2	p.P258A	1	1292508	C	T	Missense	81	23.0%		0.87847	0.87847	0.87847	Subclonal	N						Passenger	No	No	No
ACC12T	PCD4BP	p.M334	1	1449170	C	T	Missense	156	14.1%		0.07633	0.07633	0.07633	Subclonal	D						Passenger	Yes	No	No
ACC12T	PRF1	p.Q296E	1	13505524	C	G	Missense	91	19.7%		0.49970	0.49970	0.49970	Subclonal	D						Passenger	No	No	No
ACC12T	LINGO4	p.R101Q	1	15174729	C	T	Missense	72	45.8%		0.95557	0.95557	0.95557	Clonal	D						Passenger	No	No	No
ACC12T	KIAA007	p.R188W	1	15888910	G	A	Missense	113	23.9%		0.64746	0.64746	0.64746	Clonal	D						Passenger	No	No	No
ACC12T	QSOX1	p.G18E	1	1596970	C	T	Missense	81	30.0%		0.81744	0.81744	0.81744	Clonal	D						Passenger	No	No	No
ACC12T	IGSF1	p.R67D	1	15990134	G	C	Missense	59	15.0%		0.30833	0.30833	0.30833	Subclonal	N						Passenger	No	No	No
ACC12T	ZNF448	p.R69C	1	1320230	C	A	Missense	81	38.1%		0.85899	0.85899	0.85899	Clonal	D						Passenger	No	No	No
ACC12T	KF2B	p.R130W	1	20597566	C	A	Missense	135	20.0%		0.08139	0.08139	0.08139	Clonal	N						Passenger	No	No	No
ACC12T	C1orf198	p.S134N	1	23097928	C	G	Missense	111	27.0%		0.87219	0.87219	0.87219	Clonal	D						Passenger	No	No	No
ACC12T	WDR4	p.R100R	1	6988932	C	G	Missense	91	32.0%		0.88869	0.88869	0.88869	Clonal	D						Passenger	No	No	No
ACC12T	C10orf90	p.R123H	1	13818314	C	T	Missense	135	28.9%		0.90254	0.90254	0.90254	Clonal	N						Passenger	No	No	No
ACC12T	COL13	p.E248R	11	88117	T	C	Missense	186	7.3%		0.16220	0.16220	0.16220	Subclonal	D						Passenger	No	No	No
ACC12T	C11orf89	p.R81L	11	191173	T	C	Missense	81	45.4%		0.969	0.969	0.969	Clonal	D						Passenger	No	No	No
ACC12T	WEE1	p.A577T	11	608854	G	A	Missense	71	25.4%		0.81	0.81	0.81	Clonal	D						Passenger	No	No	No
ACC12T	F2	p.A576E	11	608854	A	C	Missense	71	25.4%		0.81	0.81	0.81	Clonal	D						Passenger	No	No	No
ACC12T	TMEM105	p.R217T	11	8686854	C	T	Missense	50	8.0%		0.02168	0.02168	0.02168	Subclonal	D						Passenger	No	No	No
ACC12T	PKRX	p.P188S	11	1294709	C	T	Missense	183	24.0%		0.83995	0.83995	0.83995	Clonal	N						Passenger	No	No	No
ACC12T	PKCZ	p.S508R	11	1101900	C	T	Missense	110	23.0%		0.82002	0.82002	0.82002	Clonal	D						Passenger	No	No	No
ACC12T	OR10D9	p.K295D	11	12389462	A	C	Missense	71	7.0%		0.0283837	0.0283837	0.0283837	Subclonal	N						Passenger	No	No	No
ACC12T	PRDM1	p.T164M	11	12651470	A	C	Missense	29	8.0%		0.02051	0.02051	0.02051	Subclonal	D						Passenger	No	No	No
ACC12T	WNT5B	p.R202W	12	1785122	C	T	Missense	187	28.1%		0.90915	0.90915	0.90915	Clonal	D						Passenger	No	No	No
ACC12T	BCL11	p.E830K	12	2488689	C	T	Missense	59	49.2%		0.98995	0.98995	0.98995	Clonal	N						Passenger	No	No	No
ACC12T	SMIT2	p.G294H	12	2926038	C	T	Missense	59	49.2%		0.98995	0.98995	0.98995	Clonal	N						Passenger	No	No	No
ACC12T	ALX1	p.R46L	12	8667420	G	T	Missense	53	47.2%		0.95465	0.95465	0.95465	Clonal	D						Passenger	No	No	No
ACC12T	ITNA	p.N230D	12	1083170	G	C	Missense	142	28.0%		0.87327	0.87327	0.87327	Clonal	D						Passenger	No	No	Yes
ACC12T	TUBB3C	p.V434M	12	1414544	C	T	Missense	81	27.0%		0.7270031	0.7270031	0.7270031	Subclonal	N						Passenger	No	No	No
ACC12T	ZNF476	p.D59V	13	2042045	T	A	Missense	71	12.7%		0.00991	0.00991	0.00991	Subclonal	N						Passenger	No	No	No
ACC12T	COMP	p.R94C	13	2042045	T	A	Missense	71	12.7%		0.00991	0.00991	0.00991	Subclonal	N						Passenger	No	No	No
ACC12T	DMPH3	p.S496L	13	8054158	G	A	Missense	22	54.9%		0.29297	0.29297	0.29297	Clonal	D						Passenger	No	No	No
ACC12T	KLF5	p.G420D	13	7348008	G	A	Missense	197	6.1%		0.01402791	0.01402791	0.01402791	Subclonal	D						Passenger	No	No	No
ACC12T	TMEM44	p.V121R	13	8207100	G	A	Missense	102	10.0%		0.17209	0.17209	0.17209	Subclonal	D						Passenger	No	No	No
ACC12T	SFT3A	p.P36A	14	3946277	G	C	Missense	70	54.3%		0.94812	0.94812	0.94812	Clonal	N						Passenger	No	No	No
ACC12T	SRB1	p.K841T	14	4888113	G	C	Missense	63	44.0%		0.84873	0.84873	0.84873	Clonal	D						Passenger	No	No	No
ACC12T	ATRN3	p.Q336R	14	5053354	C	G	Missense	55	58.9%		0.9566	0.9566	0.9566	Clonal	P						Passenger	No	No	No
ACC12T	IGFBP3	p.Y114H	14	10585239	A	G	Missense	20	56.0%		0.01022	0.01022	0.01022	Subclonal	D						Passenger	No	No	No
ACC12T	IGFBP3	p.Y114H	14	10585239	A	G	Missense	20	56.0%		0.01022	0.01022	0.01022	Subclonal	D						Passenger	No	No	No
ACC12T	MAR2	p.A271Y	15	4382182	C	T	Missense	97	24.7%		0.81898	0.81898	0.81898	Clonal	D						Passenger	No	No	No
ACC12T	SOX11	p.S201R	15	4481190	C	T	Missense	29	10.0%		0.02051	0.02051	0.02051	Subclonal	D						Passenger	No	No	No
ACC12T	SRH	p.R442A	15	4424254	C	T	Missense	164	6.7%		0.04834901	0.04834901	0.04834901	Subclonal	D						Passenger	No	No	No
ACC12T	CCDC113	p.R81H	16	9828715	C	T	Missense	115	20.0%		0.05442	0.05442	0.05442	Clonal	N						Passenger	No	No	No
ACC12T	DHSE	p.G280D	16	1028801	C	T	Missense	71	13.0%		0.1392	0.1392	0.1392	Subclonal	D						Passenger	No	No	No
ACC12T	SPG7	p.R451P	16	1658621	G	C	Missense	24	16.7%		0.03029	0.03029	0.03029	Subclonal	D						Passenger	No	No	No
ACC12T	SDG4	p.A407T	17	1028801	C	T	Missense	97	24.0%		0.83995	0.83995	0.83995	Subclonal	D						Passenger	No	No	No
ACC12T	FRS3	p.R121H	17	818830	C																			



**Supplementary Table 5: Genomic features of Homologous Recombination Deficiency and Microsatellite Instability in the Acinic Cell Carcinomas of the breast included in this study.**

Sample	% MSI	LST score	Myriad score	NtAI Score	Indels (n)	Indels (%)	Average indel length (bp)
ACC1	3.19	4	3	5	2	2.11	4
ACC12	10.93	0	0	0	48	17.3	3.22
ACC18	0.35	24	11	23	9	8.82	12.33

%MSI, Microsatellite instability score (MSIsensor score); LST, Large-scale State Transitions; NtAI, Telomere Allelic Imbalance score; indels, insertions or deletions.